



# Bacteriophage T4 Vaccine Platform for Next-Generation Influenza Vaccine Development

Mengling Li<sup>1,2,3,4</sup>, Pengju Guo<sup>1,2,3,4</sup>, Cen Chen<sup>1,2,3,4</sup>, Helong Feng<sup>3,5</sup>, Wanpo Zhang<sup>3</sup>, Changqin Gu<sup>3</sup>, Guoyuan Wen<sup>5\*</sup>, Venigalla B. Rao<sup>6\*</sup> and Pan Tao<sup>1,2,3,4\*</sup>

<sup>1</sup> Key Laboratory of Development of Veterinary Diagnostic Products, Ministry of Agriculture, College of Veterinary Medicine, Huazhong Agricultural University, Wuhan, China, <sup>2</sup> The Cooperative Innovation Center for Sustainable Pig Production, Huazhong Agricultural University, Wuhan, China, <sup>3</sup> Division of Pathology, College of Veterinary Medicine, Huazhong Agricultural University, Wuhan, China, <sup>4</sup> Hongshan Lab, Wuhan, China, <sup>5</sup> Institute of Animal Husbandry and Veterinary Sciences, Hubei Academy of Agricultural Sciences, Wuhan, China, <sup>6</sup> Bacteriophage Medical Research Center, Department of Biology, The Catholic University of America, Washington, DC, United States

## OPEN ACCESS

### Edited by:

Corey Patrick Mallett,  
GlaxoSmithKline, United States

### Reviewed by:

Chunhong Dong,  
Georgia State University,  
United States  
Ze Chen,  
Hunan Normal University, China

### \*Correspondence:

Pan Tao  
taopan@mail.hzau.edu.cn  
Venigalla B. Rao  
rao@cua.edu  
Guoyuan Wen  
wgy\_524@163.com

### Specialty section:

This article was submitted to  
Vaccines and Molecular Therapeutics,  
a section of the journal  
Frontiers in Immunology

**Received:** 22 July 2021

**Accepted:** 24 September 2021

**Published:** 12 October 2021

### Citation:

Li M, Guo P, Chen C, Feng H, Zhang W, Gu C, Wen G, Rao VB and Tao P (2021) Bacteriophage T4 Vaccine Platform for Next-Generation Influenza Vaccine Development. *Front. Immunol.* 12:745625. doi: 10.3389/fimmu.2021.745625

Developing influenza vaccines that protect against a broad range of viruses is a global health priority. Several conserved viral proteins or domains have been identified as promising targets for such vaccine development. However, none of the targets is sufficiently immunogenic to elicit complete protection, and vaccine platforms that can enhance immunogenicity and deliver multiple antigens are desperately needed. Here, we report proof-of-concept studies for the development of next-generation influenza vaccines using the bacteriophage T4 virus-like particle (VLP) platform. Using the extracellular domain of influenza matrix protein 2 (M2e) as a readout, we demonstrate that up to ~1,281 M2e molecules can be assembled on a 120 x 86 nanometer phage capsid to generate M2e-T4 VLPs. These M2e-decorated nanoparticles, without any adjuvant, are highly immunogenic, stimulate robust humoral as well as cellular immune responses, and conferred complete protection against lethal influenza virus challenge. Potentially, additional conserved antigens could be incorporated into the M2e-T4 VLPs and mass-produced in *E. coli* in a short amount of time to deal with an emerging influenza pandemic.

**Keywords:** flu vaccine, virus-like particle, bacteriophage T4 platform, extracellular domain of matrix protein 2, phage display

## INTRODUCTION

Influenza A (Flu) virus is a highly contagious infectious agent that can cause severe respiratory disease (1, 2). Although vaccines are available, they are strain-specific and mainly target the variable head domain of viral major envelope glycoprotein, hemagglutinin (HA) (3, 4). The stalk domain of HA exhibits a degree of conservation among influenza virus strains but cannot efficiently induce antibody responses in its native state due to the immunodominance of epitopes present in the head domain (5–8). The rapid evolution of influenza viruses through antigenic drift and shift in their surface glycoproteins, HA in particular, greatly limit the effectiveness of the current vaccines (9–12). Therefore, vaccines have to be reformulated annually using reference viruses recommended by

World Health Organization, based on the information provided by the Global Influenza Surveillance Network (13).

Vaccines that provide broader protection against diverse influenza virus strains are highly desired, and remain as one of the major challenges in Flu vaccine design. Many efforts have been focused on developing such vaccines, often referred to as “universal” Flu vaccines, using the conserved viral proteins or domains (12, 14). The internal virion proteins, nucleoprotein (NP) and matrix protein 1 (M1), were mainly used as immunogens to induce cellular immune responses, particularly CD8<sup>+</sup> T cells with cross-protection against heterologous influenza viruses (15–17). Engineered headless HA stalk, in which the immunodominant head domain was removed, was mainly used to induce antibodies that recognize or neutralize diverse influenza virus strains (18, 19). Another widely used target for universal Flu vaccines is the extracellular domain of matrix protein 2 (M2e) that is highly conserved among divergent influenza virus strains (14, 20, 21). However, none of these vaccine targets are highly immunogenic and many strategies were employed to enhance their immunogenicity (22–25).

By taking advantage of *in vitro* assembly of antigen proteins on bacteriophage T4 capsid, we recently developed a virus-like nanoparticle (VLP) platform that can elicit robust immune responses against a variety of displayed antigens, without any adjuvants (26, 27). In this study, we aimed to develop an M2e-based influenza vaccine using this T4 VLP platform. The immunogenicity of M2e, a NH<sub>2</sub>-terminal 23-residue peptide of viral matrix protein 2 (M2), is otherwise quite low during natural infection due to its small size and low abundance on the virion surface (28). However, when displayed on a VLP, the M2e induced significant immune responses and provided variable protection against influenza virus infection (29, 30). Although many different platforms such as hepatitis B virus core particle (31), human papillomavirus particle (32), and tobacco mosaic virus (33) were used as VLP carriers for M2e, phage-based VLP platforms are more attractive for their cost-effectiveness and large-scale manufacturing potential that is critical during an influenza pandemic.

Several phage platforms have been tested for M2e Flu vaccine design. The M2e antigens displayed on T7 phage capsids, though immunogenic, failed to provide complete protection against lethal influenza virus challenge (34). This was probably due to the low copy number of M2e molecules on the phage capsid. Indeed, it was found that vaccines with higher M2e epitope densities resulted in higher protection efficacy (35, 36), and most of the licensed viral vaccines contain high density of antigens on the virion surface (37). Although phage fd can display up to 2,700 copies of peptide per capsid through its major coat protein pVIII, the display is sensitive to the size of the peptide (38). Therefore, only part of M2e (residues 2–16) could be displayed on phage fd, which still provided protection from death but the challenged mice showed severe body weight loss indicating its limited value as a vaccine (39).

We have previously reported that phage T4 can be used for efficient display of full-length proteins as large as 120 kDa at high density because of its unique capsid architecture (40). The 120 ×

86 nm phage capsid is comprised of four major capsid proteins: two essential proteins, the capsid shell protein gp23\* (930 copies) and the vertex protein gp24\* (55 copies), and two non-essential proteins, the small outer capsid protein (Soc, 870 copies) and the highly antigenic outer capsid protein (Hoc, 155 copies) (**Figure 1A**) (26, 41). Deletion of Hoc and Soc (Hoc<sup>-</sup>Soc<sup>-</sup> T4) has no effect on the propagation of T4 under laboratory conditions, and recombinant antigens fused to Hoc or Soc specifically bind to Hoc<sup>-</sup>Soc<sup>-</sup> T4 capsids *in vitro* with high affinity (26, 27, 42, 43).

Here, we show that three variants of M2e peptide from human, swine, and avian influenza viruses tandemly fused to the COOH-terminus of Soc can be efficiently displayed on Hoc<sup>-</sup>Soc<sup>-</sup> T4 capsids at high density by *in vitro* assembly (**Figure 1**). The resultant M2e-decorated T4 nanoparticles are found to be highly immunogenic and induced complete protection against lethal influenza virus challenge, without any adjuvant. Importantly, the vaccinated mice showed no or minor symptoms after lethal influenza virus challenge, based on clinical observations including body weight and pathological analyses. These studies provide proof-of-concept for the development of next-generation influenza vaccines using the phage T4 VLP platform.

## RESULTS

### Construction of M2e-Decorated Bacteriophage T4 Nanoparticles

To stimulate increased breadth of immunogenicity and protection against Flu viruses, a 3M2e gene containing three types of M2e sequences from human, swine, and avian influenza viruses were synthesized (**Supplementary Table**) and fused to the COOH-terminus of Soc to generate Soc-3M2e. A flexible GGSSGGSS linker was introduced between each M2e segment as depicted in **Figure 1B**, to minimize any interference in the folding of the M2e domains. Hexa-histidine tags were also added to both termini of the Soc-3M2e protein. The fusion protein was expressed in *E. coli* and purified by Ni<sup>2+</sup> affinity chromatography followed by size-exclusion chromatography. The major peak corresponding to a molecular weight of ~21.8 kDa (monomeric Soc-3M2e) was collected (**Figure 1B**, blue profile). The purity of the recombinant Soc-3M2e proteins was confirmed by sodium dodecyl sulfate–polyacrylamide gel electrophoresis (SDS-PAGE), which showed a single major band with a molecular mass of ~22 kDa, equivalent to the Soc-3M2e fusion protein (**Figure 1B**).

The 3M2e-decorated T4 nanoparticles (3M2e-T4 nanoparticles) were prepared by incubation of the purified Soc-3M2e protein with the CsCl-purified Hoc<sup>-</sup>Soc<sup>-</sup> T4 phages as previously described (44) (**Figure 1C**). To optimize the copy number of 3M2e, ~5 × 10<sup>10</sup> T4 phages were incubated with different quantities of the Soc-3M2e protein (**Figure 1C**). The presence of bound Soc-3M2e was determined by SDS-PAGE analysis of 3M2e-T4 nanoparticles isolated by high-speed centrifugation. The data show that the Soc-3M2e protein bound efficiently to the Hoc<sup>-</sup>Soc<sup>-</sup> T4 phages, even at a 1:1 ratio

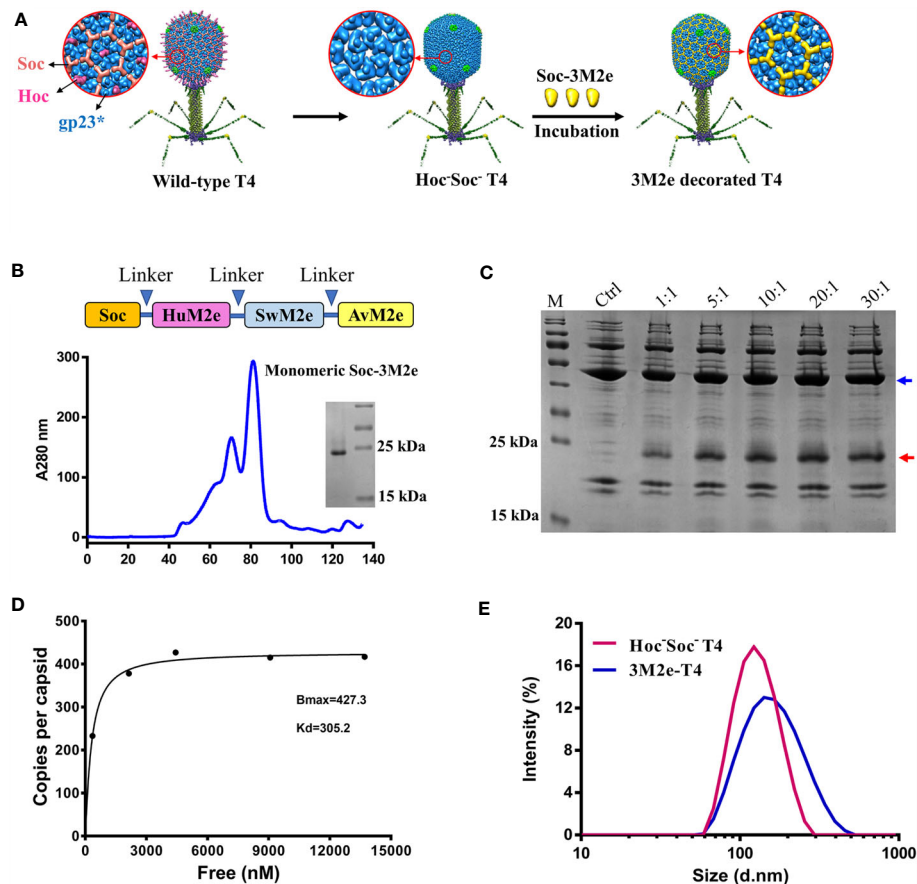


**FIGURE 1** | Construction of 3M2e-T4 VLPs. **(A)** schematic diagram of 3M2e-T4 VLPs preparation. Structural models of wild-type T4 and Hoc<sup>-</sup>Soc<sup>-</sup> T4 phages were shown. 3M2e decorated T4 nanoparticles were prepared by incubation of Soc-3M2e proteins with Hoc<sup>-</sup>Soc<sup>-</sup> T4 phages as described in Materials and Methods. **(B)** Purification of Soc-3M2e. Soc-3M2e fusion was constructed by fusing 3M2e, which contains three tandem copies of M2e from human, swine, and avian influenza viruses, to the COOH-terminus of Soc. Arrows indicated the flexible linkers (GGSSGGSS) between each component. Soc-3M2e protein was purified by HisTrap affinity chromatography followed by size exclusion chromatography. Only the monomeric peak was collected, and the purity of Soc-3M2e protein was analyzed by SDS-PAGE. **(C)** Assembly of 3M2e-T4 VLPs *in vitro*. About  $5 \times 10^{10}$  Hoc<sup>-</sup>Soc<sup>-</sup> T4 phages were incubated with at the indicated ratios of Soc-3M2e protein molecules to capsid binding sites (see Materials and Methods for the details). 3M2e-T4 VLPs were analyzed by SDS-PAGE. The same amount of Hoc<sup>-</sup>Soc<sup>-</sup> T4 phages was used as a control. Blue and red arrows indicated gp23\* and Soc-3M2e, respectively. **(D)** Saturation binding curve of Soc-3M2e. The bound and unbound (not shown) Soc-3M2e proteins were calculated using BSA a standard. The copy numbers of Soc-3M2e per capsid were determined using gp23\* as internal control. The data were plotted as one-site saturation ligand binding curve. **(E)** The diameter distributions of Hoc<sup>-</sup>Soc<sup>-</sup> T4 (red line) and 3M2e-T4 nanoparticles (blue line).

of Soc-3M2e molecules to Soc binding sites, and reached saturation at ratio of 10:1 (**Figure 1C**). The copy number of bound Soc-3M2e per capsid ( $B_{max}$ ) calculated from the binding curve was 427, and the apparent binding constant ( $K_d$ ) was 305 nM (**Figure 1D**). Since each Soc-3M2e protein contains three tandem copies of M2e peptide, there are ~1,281 M2e molecules assembled on each T4 nanoparticle, which is remarkably higher than any VLPs reported so far. The diameter distribution and zeta-potential of 3M2e-T4 nanoparticles was determined using Zetasizer Nano ZS. The average diameter of 3M2e-T4 nanoparticles is 150.9 nm, which is larger than the diameter of Hoc<sup>-</sup>Soc<sup>-</sup> T4 phages (mean = 120.8 nm) (**Figure 1E**), indicating the binding of Soc-3M2e. We didn't observe significant difference in zeta-potentials between Hoc<sup>-</sup>Soc<sup>-</sup> T4 ( $-26.7 \pm 0.4$  mV) and M2e-T4 nanoparticles ( $-24.3 \pm 0.12$  mV) (**Figure S1**).

### 3M2e-T4 Phage Nanoparticles Induced Robust M2e-Specific Antibodies

To determine the immunogenicity of 3M2e-T4 nanoparticles, mice were intramuscularly immunized with 3M2e-T4 nanoparticles displaying a total of 15 $\mu$ g 3M2e antigen on day 0, 14, and 28 (**Figure 2A**). Mice immunized with PBS, 15 $\mu$ g of Soc-3M2e soluble proteins, or a simple mixture of 15 $\mu$ g Soc-3M2e antigen and the same number of T4 phage nanoparticles (Soc-3M2e+T4) were used as controls. To minimize binding prior to immunization, the Soc-3M2e antigen was mixed with phage T4 at the time of immunization (most of the Soc-3M2e did not bind to capsid, see Materials and Methods for the details). Sera were collected according to the scheme shown in **Figure 2A**, and the titers of M2e-specific antibodies were determined by enzyme-linked immunosorbent assay (ELISA). All mice

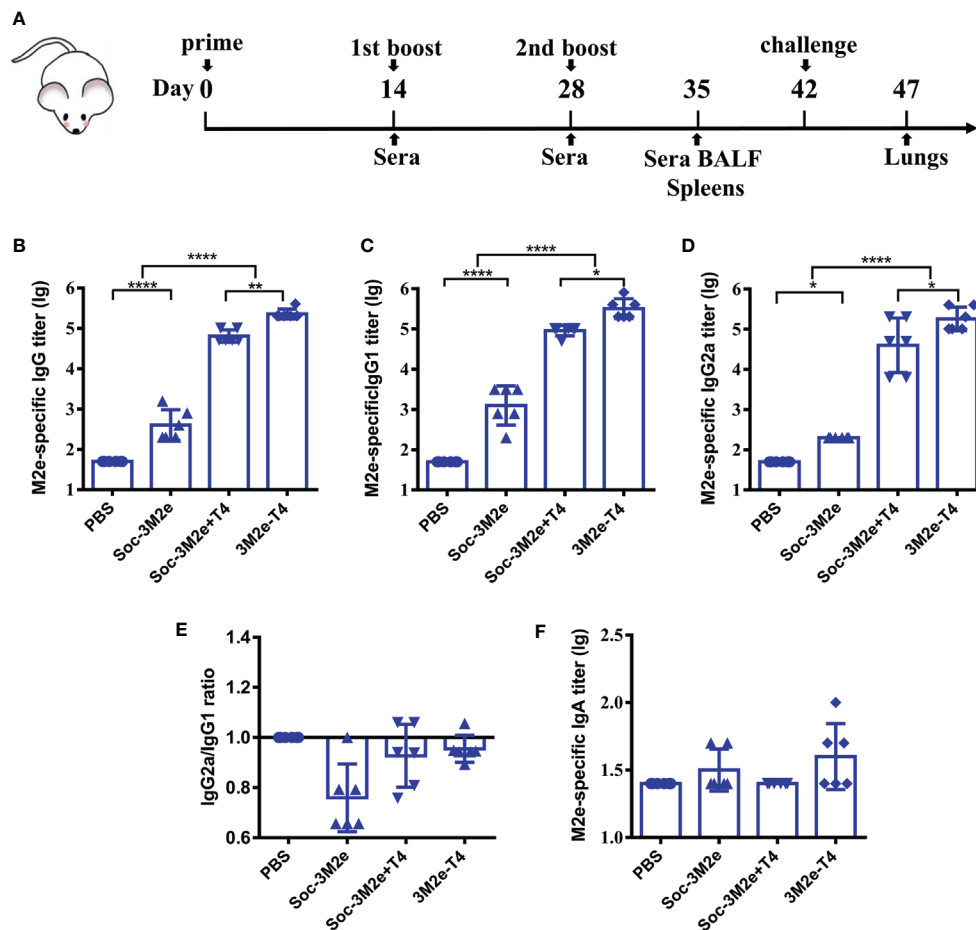


**FIGURE 2** | M2e-specific humoral immune responses. **(A)** Scheme of mouse immunization. Sera were obtained before each immunization. The titers of M2e-specific IgG **(B)**, IgG1 **(C)**, IgG2a **(D)**, and IgA **(F)** were determined by ELISA using peptides pool of M2e from human, swine, and avian influenza viruses. **(E)** Ratio of M2e-specific IgG2a to IgG1 were calculated. Data were shown as means  $\pm$  S.D. \*, \*\*, and \*\*\*\* indicated  $p < 0.05$ ,  $p < 0.01$ , and  $p < 0.0001$  respectively (ANOVA).

immunized with PBS were negative for M2e-specific IgG even at a low sera dilution of 50. The Soc-3M2e soluble proteins induced very low levels of M2e-specific IgG antibodies. However, 3M2e-T4 nanoparticles, without any adjuvant, induced very high levels of 3M2e-specific IgG antibodies, with end point titers of  $\sim 4 \times 10^5$  (Figure 2B). Even a simple mixture of Soc-3M2e and T4 phage (Soc-3M2e+T4 mixture) generated high titers ( $\sim 1 \times 10^5$ ) of M2e-specific antibodies when compared to the very low titers generated by the soluble Soc-3M2e antigen (Figure 2B,  $p < 0.0001$ , ANOVA). These data point to the remarkable immune stimulatory effect of the T4 phage nanoparticles.

Since M2e-induced immune protection mainly depends on antibody-dependent cellular cytotoxicity (ADCC) and antibody-dependent cellular phagocytosis (ADCP), the efficiencies of which are different between IgG subtypes (45–47), we determined the titers of M2e-specific IgG1 ( $T_H2$ -biased) and IgG2a ( $T_H1$ -biased). The Soc-3M2e soluble antigen mainly induced IgG1 antibodies, whereas mice immunized with 3M2e-T4 nanoparticles or Soc-3M2e+T4 mixture produced similar levels of both IgG1 and IgG2a

antibodies (Figures 2C–E). Elicitation of balanced  $T_H1$  and  $T_H2$  biased immune responses is a significant feature of the T4 vaccine delivery platform and generally important for protection against infectious disease. We have also determined the 3M2e-specific IgA antibodies in sera. Although 3M2e-T4 nanoparticles induced IgA antibodies in some of the mice, the data were not statistically significant ( $p > 0.05$ , ANOVA, Figure 2F).

### 3M2e-T4 Nanoparticle-Induced Anti-M2e Antibodies Bind to Influenza Virions and Influenza Virus-Infected Cells

To determine whether 3M2e-T4 nanoparticles induced antibodies recognize M2e on influenza virions, A/Puerto Rico/8/34 (H1N1) virus was inactivated with  $\beta$ -propiolactone and used as the coating antigen in ELISA assays. The data revealed that these antibodies, regardless of the IgG subtype, specifically bound to the influenza virions (Figures 3A–C). Consistent with the end point titers (Figure 2), balanced levels of virion-binding titers were observed for both the IgG1 and IgG2a subtypes. As



expected, sera from PBS immunized mice showed negative results even at a low sera dilution of 10 (Figures 3A–C). Since M2e-induced immune protection mainly depends on ADCC and ADCP, we then examined whether M2e presented in plasma membranes of influenza virus-infected cells can be recognized by 3M2e-T4 induced antibodies. Madin-Darby canine kidney (MDCK) cells infected with A/Puerto Rico/8/34 (H1N1) influenza virus at a multiplicity of infection (MOI) of 1 were tested for the binding of M2e-specific antibodies by indirect immunofluorescence assay (Figure 3D). The data indicated that the sera from 3M2e-T4 VLPs immunized mice showed significant binding to influenza virus-infected cells, but not to mock-treated cells (Figure 3D). Together, these data demonstrated that the 3M2e-T4 nanoparticle can efficiently induce M2e-specific antibodies that recognize M2e presented both on influenza virions and on virus-infected cells, indicating their potential protection against influenza virus infection.

### 3M2e-T4 Nanoparticles Elicit Strong Cellular Immune Responses

To investigate whether the 3M2e-T4 nanoparticles elicited M2e-specific cellular immune responses, mice were sacrificed 7 days

after the second boost, and spleens were collected to isolate peripheral blood mononuclear cells (PBMCs). The number of IFN- $\gamma$  and IL-4 secreting cells were analyzed by ELISPOT using 10 $\mu$ g/ml M2e peptide as a stimulus. Neither the mice immunized with Soc-3M2e soluble antigen nor those immunized with the Soc-3M2e+T4 mixture generated IFN- $\gamma$  and IL-4 secreting cells, while the mice immunized with 3M2e-T4 nanoparticles generated significant numbers of M2e-specific IFN- $\gamma$  (Figure 4A) and IL-4 secreting cells (Figure 4B). These data demonstrate that assembly of 3M2e on T4 nanoparticles is essential to stimulate the cellular arm of the host immune system. This seems to be not that critical for the humoral arm because, as shown above, substantial induction of antibodies was evident with the Soc-3M2e+T4 mixture (Figures 2B–D).

### 3M2e-T4 Nanoparticles Elicited M2e-Specific Mucosal Antibodies

The mucosal surfaces of the respiratory tract are major ports of entry for influenza viruses, and previous studies indicated that both mucosal IgG and serum IgG are conducive for efficient protection (48). To determine if the 3M2e-T4 nanoparticles stimulated mucosal antibodies, bronchoalveolar lavage fluid

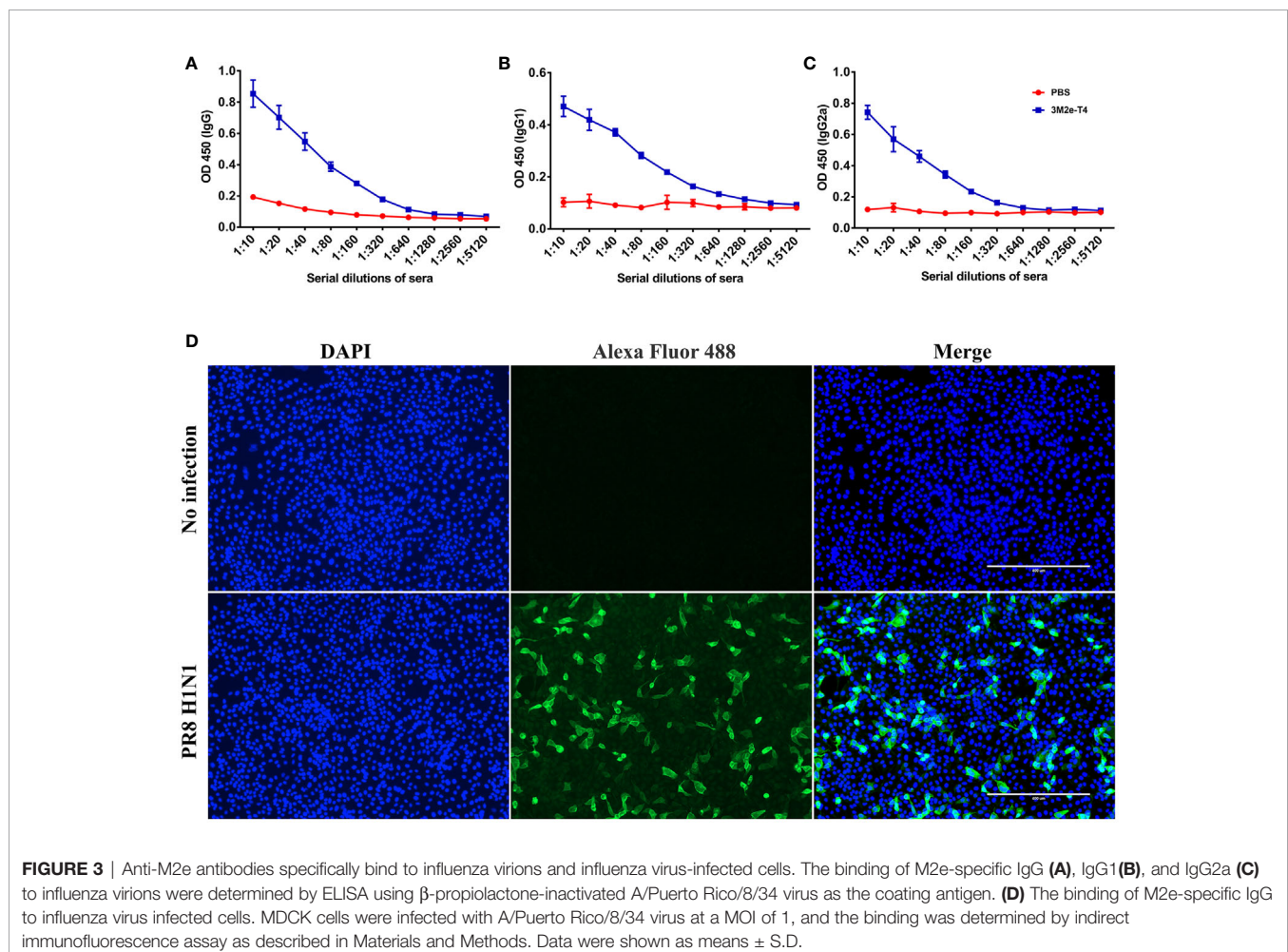


**FIGURE 3** | Anti-M2e antibodies specifically bind to influenza virions and influenza virus-infected cells. The binding of M2e-specific IgG (A), IgG1 (B), and IgG2a (C) to influenza virions were determined by ELISA using  $\beta$ -propiolactone-inactivated A/Puerto Rico/8/34 virus as the coating antigen. (D) The binding of M2e-specific IgG to influenza virus infected cells. MDCK cells were infected with A/Puerto Rico/8/34 virus at a MOI of 1, and the binding was determined by indirect immunofluorescence assay as described in Materials and Methods. Data were shown as means  $\pm$  S.D.

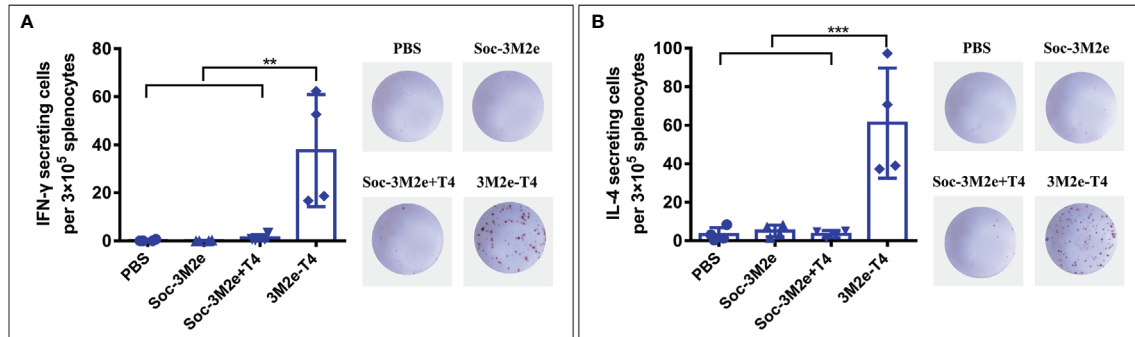


**FIGURE 4** | M2e-specific cellular immune responses. Mice ( $n = 4$ ) were immunized according to the scheme shown in **Figure 2A**, and splenocytes were isolated on day 35. The IFN- $\gamma$  (**A**) and IL-4 (**B**) secreting lymphocytes were assayed by ELISPOT as described in Materials and Methods. The right images of each panel show the representative results of ELISPOT wells from each group. Data were represented as mean  $\pm$  S.D. of four mice in each group. \*\* $p < 0.01$ ; \*\*\* $p < 0.001$  (ANOVA).

(BALF) was collected 7 days post last immunization, and the presence of IgG and IgA antibodies were detected using ELISA. As shown in **Figure 5A**, soluble Soc-3M2e was able to induce low levels of M2e-specific IgG antibodies, whereas the 3M2e-T4 nanoparticles induced the highest levels. As in the case of serum IgG, the Soc-3M2e+T4 mixture could also induce mucosal IgG, much higher than the soluble antigen. As expected, the PBS control mice had no detectable levels of anti-M2e IgG antibodies (**Figure 5A**). Subtype analysis of the IgG antibodies showed that Soc-3M2e soluble antigens only elicited M2e-specific mucosal IgG1, whereas mice immunized with 3M2e-T4 nanoparticles or Soc-3M2e+T4 mixture induced balanced levels of both mucosal IgG1 and IgG2a antibodies (**Figures 5B, C**). However, all the groups failed to develop M2e-specific IgA antibodies in BALF (**Figure 5D**).

### 3M2e-T4 Nanoparticles Provided Complete Protection Against Influenza A Virus Challenge

To evaluate the protective efficacy of each formulation, immunized mice were challenged with 5LD<sub>50</sub> of A/Puerto Rico/8/34 (H1N1) virus and monitored daily for body weight

and survival for 14 days. As shown in **Figure 6A**, infection of influenza virus resulted in substantial weight loss of PBS control mice, or mice immunized with either the Soc-3M2e soluble antigen, or Soc-3M2e+T4 mixture, three days post infection. All the mice in the PBS control group died 10 days post challenge and five of the six mice immunized with the soluble Soc-3M2e died 9 days post challenge (**Figure 6B**), whereas 67% of the mice vaccinated with Soc-3M2e+T4 mixture recovered and survived (**Figure 6B**). In contrast, all the mice immunized with 3M2e-T4 nanoparticles not only survived the lethal challenges with the H1N1 virus infections (**Figure 6B**), but also, remarkably, showed no significant body weight loss (**Figure 6A**).

The protection efficacy was further evaluated by pathological analysis of the lungs of the immunized mice 5 days post-challenge. **Figure 6C** shows representative results of the lung lesions (column I) and pathological changes of alveoli (column II), bronchi (column III), and pulmonary vessels (column IV). Overall, mice immunized with Soc-3M2e+T4 mixture showed obvious, though less severe, lesions in the lungs when compared to the PBS control mice or mice immunized with soluble Soc-3M2e antigen, whereas no obvious lesions were found in 3M2e-T4 nanoparticle immunized mice (column I). The alveolar walls

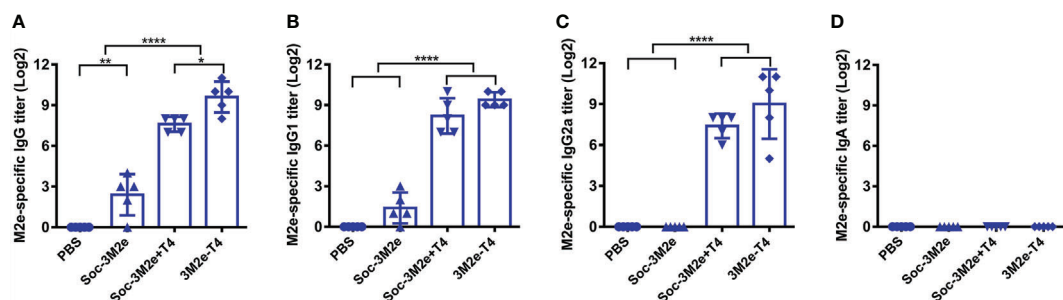


**FIGURE 5** | M2e-specific antibodies in BALF. Bronchoalveolar lavage fluids were collected 7 days after last immunization ( $n = 5$ ). M2e-specific total IgG (**A**), IgG1 (**B**), IgG2a (**C**), and IgA (**D**) were determined by ELISA using a mixture of human, swine, avian influenza virus M2e peptides as the capture antigen (2  $\mu$ g/ml). Data were presented as means  $\pm$  S.D. \* $p < 0.05$ ; \*\* $p < 0.01$ ; \*\*\*\* $p < 0.0001$  (ANOVA).

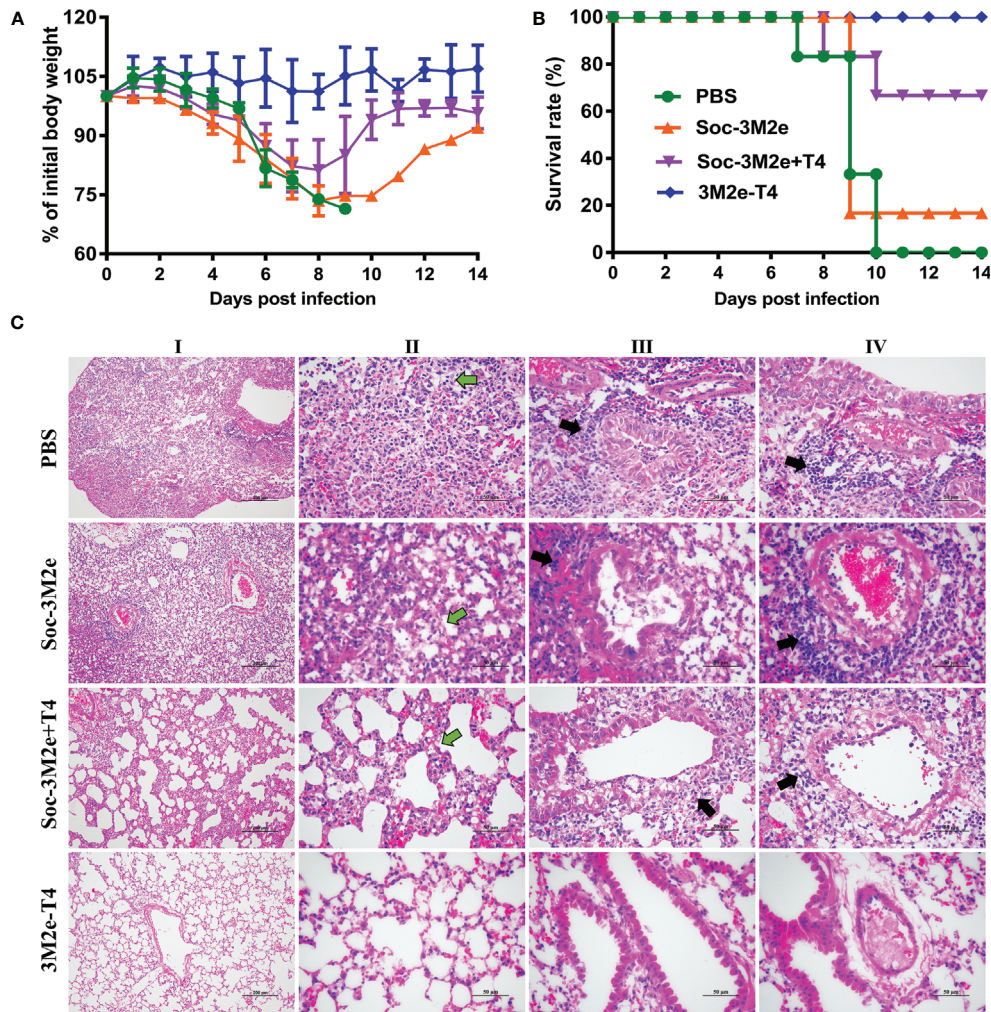


**FIGURE 6** | 3M2e-T4 VLPs provided complete protection against influenza virus challenge. Mice ( $n = 6$ ) were challenged with  $5 \times LD_{50}$  of A/Puerto Rico/8/34 two weeks after last immunization. Weight loss (**A**) and survival rate (**B**) of mice were monitored daily for 14 days. (**C**) Pathological analysis of lungs from mice ( $n = 3$ ) challenged with virus was carried out in a separate experiment, in which mice were immunized with the same immunization procedure described above. Five days post infection with  $5 \times LD_{50}$  of A/Puerto Rico/8/34, mice were euthanized, and lung sections were prepared as described in Materials and Methods. The representative results from each group were shown (column I, scale bar, 200  $\mu\text{m}$ ; Columns II-IV, scale bar, 50  $\mu\text{m}$ ). Main pathological changes are thickening of alveolar septa of mice (column II, green arrows), inflammatory cells infiltrated around the bronchi (column III, black arrows), and pulmonary blood vessels (column IV, black arrows).

of PBS or soluble Soc-3M2e immunized mice were severely thickened (column II), and a large number of inflammatory cells infiltrated around the bronchi (column III) and pulmonary blood vessels (column IV). Mice immunized with Soc-3M2e+T4 mixture also exhibited similar but less severe pathological changes. However, in contrast, the mice vaccinated with 3M2e-T4 nanoparticles showed relatively normal alveolar wall thickness and negligible inflammatory infiltration (**Figure 6C**).

## DISCUSSION

The influenza virus M2e antigen is considered to be an attractive target for the development of universal influenza vaccines

(49–51). However, VLP carriers and/or adjuvants are absolutely needed for designing the M2e-based vaccines because of the poor immunogenicity of the M2e peptides. By taking advantage of the phage T4 nanoparticle platform, in this study, we developed a novel 3M2e-T4 VLP vaccine that, without any adjuvant, induced robust humoral and cellular immune responses and provided complete protection against influenza virus challenge.

The 3M2e-T4 nanoparticles were prepared by simply incubating the Soc-3M2e fusion protein with Hoc<sup>+</sup>Soc<sup>-</sup> T4 phages, both of which can be produced in large-scale in *E. coli*. Therefore, our M2e-T4 nanoparticles provide an approach to manufacture influenza vaccines in a short amount of time, which is critical to deal with an emerging influenza pandemic. The



3M2e-T4 nanoparticles can be stored at 4°C for at least 6 days without significant degradation of the bound antigen (**Figure S2**), and it can also be lyophilized for long-term storage. Although phages T7 and fd have previously been used as carriers to present M2e, they conferred limited protection (34, 39). This is probably because these platforms cannot present full-length M2e peptides at high density, which is a key determinant for inducing strong and protective immune responses (52). Our data demonstrated that each T4 phage nanoparticle was decorated with ~427 copies of the 21.8 kDa Soc-3M2e, and each copy containing three tandem repeats of M2e peptide from human, swine, and avian influenza viruses. This means that ~1,281 copies of M2e molecules were presented on a 120 x 86 nm nanometer capsid particle, the highest density reported so far on any VLP. Such high density as well as the repetitive and symmetrical arrangement of M2e epitopes mimicking the surface structure of a viral pathogen, probably led to robust stimulation of the host immune system eliciting strong immune responses without the need for an adjuvant.

Apart from high epitope density, the high immunogenicity of 3M2e-T4 VLPs might also be because the T4 phage was able to stimulate innate immune responses and may have natural adjuvant properties (26, 38). Indeed, a mixture of Soc-3M2e antigen and T4 phages (Soc-3M2e+T4) in which most of the antigen was not attached to capsid induced quite high levels of M2e-specific antibodies in sera (**Figures 2B–D**) and BALF (**Figure 5**). Importantly, however, the 3M2e-T4 nanoparticles elicited the strongest immune responses. This might be because display of 3M2e on T4 phage represents linkage of antigen to an adjuvant-loaded delivery system, which ensures simultaneous presentation of both to the same immune cell such as the antigen-presenting cells (APCs) that could significantly enhance the immune responses (53). T4 phages also induced vector-specific antibodies after immunization (**Figure S3A**), which could be a concern of T4 VLP platform. However, such antibodies did not interfere the immunogenicity of 3M2e displayed on T4 nanoparticles based on the observation that M2e-specific antibodies were boosted significantly after second and third immunizations (**Figure S3B**). This might be because T4 phage is mainly used as a scaffold to efficiently deliver and present antigens to immune system, and it cannot replicate in mice as some other live viral vectors. The efficacy of such live viral vaccines depends on their replication *in vivo* to produce enough antigens, which might be inhibited by vector-specific immune responses. Our data indicated that the T4 vector immunogenicity is not a significant issue in the case of T4 VLP vaccines.

Unlike soluble Soc-3M2e protein that mainly elicited Th2-biased responses, the 3M2e-T4 VLPs induced balanced T<sub>H</sub>1 and T<sub>H</sub>2 immune responses (**Figures 2E, 4**), which is vital for vaccine efficacy. T<sub>H</sub>1-type cytokines such as IFN- $\gamma$  tend to induce the proinflammatory responses, which could lead to tissue damage. T<sub>H</sub>2-type cytokines such as IL-4 are mostly involved in mediating anti-inflammatory response, which will counteract the excessive microbicidal effect mediated by T<sub>H</sub>1-based responses (54–56). Our results showed that mice immunized with 3M2e-T4 VLPs, but not soluble Soc-3M2e proteins, induced

similar levels of M2e-specific IgG1 and IgG2a (**Figure 2E**). Similar results were also observed for the M2e-specific IFN- $\gamma$  and IL-4 secreting cells (**Figure 4**) indicating that M2e-T4 VLPs facilitate both T<sub>H</sub>1-type and T<sub>H</sub>2-type immune responses. Additionally, M2e-specific antibodies generally are non-neutralizing and their protection is mainly dependent on antibody-dependent cellular cytotoxicity (ADCC) and antibody-dependent cellular phagocytosis (ADCP) (45–47, 57). Therefore, high levels of M2e-specific IgG2a antibodies, which are more potent than other IgG subclasses in directing ADCC, are desirable for M2e-based vaccines.

Previous studies have suggested that T-cell responses induced by M2e vaccines also contributed to the protection against influenza infections (49, 58). In our current study, we found that the 3M2e-T4 VLPs, but not the soluble Soc-3M2e or a mixture of T4 and Soc-3M2e, elicited high levels of M2e-specific IFN- $\gamma$  and IL-4 secreting lymphocytes in the spleens of vaccinated mice. These might have contributed to the enhanced protections of 3M2e-T4 VLPs (**Figure 6**), and the expectation is that, since we have used three versions of M2e and that M2e as such is highly conserved among influenza viruses, these responses would afford cross-protection to diverse viruses belonging to different subtypes.

Although M2e-based universal influenza vaccines are promising, it is highly desirable to include other conserved antigens such as HA-stalk, NP, and M1 to cover a broad range of virus types. Other than displaying M2e on capsids, our T4 vaccine platform provides flexibility and capacity for next-generation multivalent vaccine design. For instance, we have demonstrated that the T4 platform can be used to simultaneously display and deliver different kinds of protein antigens or DNAs encoding antigen proteins, target antigens to dendritic cells, and co-deliver antigens and molecular adjuvants (27, 38, 40). Therefore, potent multivalent T4-Flu VLP vaccines can be designed and experiments are currently underway to develop such next-generation broadly effective Flu vaccines.

In conclusion, our studies demonstrated that the T4 phage nanoparticles displaying the Flu viral M2e peptides at high density, without the inclusion of an external adjuvant, stimulate strong humoral and cellular immune responses in mice against the virion-exposed M2e that is otherwise poorly immunogenic. These responses also afforded complete protection against lethal Flu virus challenge. These results, thus, provide a proof-of-concept for the development of potent next-generation influenza vaccines using the T4 VLP platform by incorporating additional conserved influenza antigens and other immunostimulatory molecules.

## MATERIALS AND METHODS

### Ethics Statement

All animal experiments were approved by the Research Ethics Committee (HZAUMO-2021-0023), Huazhong Agricultural University, Hubei, China and performed in the Laboratory Animal Center of Huazhong Agricultural University strictly in



accordance with the Guidelines for the Care and Use of Laboratory Animals, Huazhong Agricultural University.

## Construction of Plasmids

The plasmid pET-RbSoc was constructed by inserting Soc gene of RB69 phage into pET28b expression vector using NheI and XhoI restriction sites. The 3M2e gene (Table S1) encoding three tandem copies of M2e from human, swine, and avian influenza viruses separated by two flexible linkers (GGSSGGSS) was synthesized and cloned into pUC19 vector using SalI and XhoI restriction sites. The 3M2e gene fragment was cut from pUC19 plasmid using SalI and XhoI and subcloned into pET-RbSoc plasmid at the XhoI site to generate the expression plasmid pRbSoc-3M2e, in which the 3M2e gene was fused to COOH-terminus of RB69 Soc.

## Purification of Recombinant Soc-3M2e Protein

The pRbSoc-3M2e expression plasmid was transformed into *E. coli* BL21 (DE3) competent cells (Novagen), and a single colony was cultured overnight in LB medium supplemented with 50 µg/ml kanamycin. Ten ml of the overnight culture was inoculated into 1 L of fresh LB medium containing the antibiotic, and the expression of Soc-3M2e was induced with 1mM isopropyl-β-D-thiogalactoside (IPTG) at 30°C for 2 hours when the OD600 of culture reached 0.8. *E. coli* cells were collected by centrifugation at 4,300g for 15 min and resuspended with binding buffer (20 mM Tris-HCl pH 8.0, 100 mM NaCl, 10 mM imidazole, and 5 µg/ml DNase I). The cells were lysed by high-pressure cell disruptor at 4°C, and cell debris was removed by high-speed centrifugation (35,000g, 20 min, 4°C). The supernatant containing the recombinant Soc-3M2e proteins was passed through a 0.22 µm filter and loaded onto HisTrap column (Yeasen, Shanghai, China). After washing with 40 ml washing buffer (20 mM Tris-HCl pH 8.0, 100 mM NaCl, and 20 mM imidazole), the Soc-3M2e protein was eluted with elution buffer (20 mM Tris-HCl pH 8.0, 100 mM NaCl, and 400 mM imidazole). The peak fractions were collected and further purified by size-exclusion chromatography (Hi-load 16/60 Superdex 200 column, GE Healthcare Life Sciences) using gel filtration buffer (20 mM Tris-HCl pH 8.0, 100 mM NaCl). The purity of eluted Soc-3M2e protein was analyzed by SDS-PAGE, and protein concentration was determined with BSA as a standard. The endotoxin level present in purified Soc-3M2e protein was 0.05 EU/ml tested using Limulus Amebocyte Lysate (LAL) Endotoxin Quantitation Kit (Xiamen Bioendo Technology Co., Ltd, Xiamen China).

## T4 Phage Purification

The propagation and purification of Hoc<sup>-</sup>Soc<sup>-</sup> phage T4 were carried out as previously described (44, 59, 60). Briefly, an overnight culture of *E. coli* P301 was inoculated into LB/M9CA medium and incubated at 37°C until the cell density reaches 1.5–2.0 × 10<sup>8</sup> cells/ml. *E. coli* cells were then infected with Hoc<sup>-</sup>Soc<sup>-</sup> phage T4 at a multiplicity of infection (MOI) of 0.2–0.4, and cultured at 37°C for another 2–3 h. The cultures were harvested

by centrifugation at 30,000g for 30 min, and the pellet containing phages was suspended in Pi-Mg buffer (26 mM Na<sub>2</sub>HPO<sub>4</sub>, 22 mM KH<sub>2</sub>PO<sub>4</sub>, 79 mM NaCl, 1 mM MgSO<sub>4</sub>) containing chloroform and DNase I. After 20 min incubation at 37°C, the suspension was centrifuged at 4,300g for 20 min to remove cell debris, and phages in the supernatant were collected by high-speed centrifugation (30,000g, 30 min). The phage pellet was resuspended in 1 ml Pi-Mg buffer and purified by CsCl step density gradient centrifugation. Finally, the phages were dialyzed against dialysis solution I (10 mM Tris pH 8.0, 200 mM NaCl, and 5 mM MgCl<sub>2</sub>) for 5 h followed by dialysis solution II (10 mM Tris pH 8.0, 50 mM NaCl, and 5 mM MgCl<sub>2</sub>) for overnight at 4°C. The endotoxin level present in purified Hoc<sup>-</sup>Soc<sup>-</sup> phages was 1.53 EU/ml, which is well under the maximum recommended endotoxin levels, 20 EU/ml, in subunit vaccines (61).

## Assembly of 3M2e Antigens on Hoc<sup>-</sup>Soc<sup>-</sup> T4 Capsids *In Vitro*

*In vitro* assembly of proteins on Hoc<sup>-</sup>Soc<sup>-</sup> T4 phages was performed as described previously (26, 44). To optimize the binding of Soc-3M2e, about 5 × 10<sup>10</sup> phage particles were incubated at 4°C for 45 min with Soc-3M2e proteins at different ratios of antigen molecules to Soc binding sites (1:1 to 30:1, Figure 1C). The unbound Soc-3M2e proteins were removed by centrifugation at 21,130 g for 30 min, and the pellet of phage particles containing bound proteins were washed twice with PBS. The Soc-3M2e decorated phage particles were finally resuspended in PBS, transferred to a new tube, and analyzed by SDS-PAGE. The gp23\* and Soc-3M2e proteins in each lane were quantified by Image-Pro Plus software using BSA as a standard. The copy number of bound Soc-3M2e proteins was determined using gp23\* (49 kDa, 930 copies per capsid) as internal control. The saturation binding curve was generated using Prism GraphPad software as previously described (26, 27, 43). The y-axis showed the copy number at the different ratios, while x-axis represented the concentration of unbound Soc-3M2e. The apparent binding affinity (K<sub>d</sub>) and the maximal number of bound molecules (B<sub>max</sub>) were determined by nonlinear regression analysis with the methods of one site specific binding with a Hill slope. The diameter distribution and zeta-potential of the nanoparticles were determined using Zetasizer Nano ZS (Malvern Panalytical, UK).

## Immunizations and Influenza A Virus Challenge

Six- to eight-week-old female BALB/c mice were purchased from Laboratory Animal Center of Huazhong Agricultural University, Hubei, China. The 3M2e-T4 nanoparticles were prepared as described above and injected intramuscularly into mice (15µg 3M2e per dose) at week 0, 2, and 4. Each batch of sample was analyzed by SDS-PAGE for consistency in the copy number of displayed antigens before injection (Figure S4). Mice immunized with the mixture of Soc-3M2e proteins (15µg 3M2e per dose) and T4 phages (9 × 10<sup>11</sup> particles) were used as controls (Soc-3M2e+ T4). To minimize the binding of Soc-3M2e, the protein was mixed with T4 phages right before each immunization.

Other control groups included PBS, Soc-3M2e soluble proteins (15 µg 3M2e per dose), and T4 phages ( $9 \times 10^{11}$  particles). Two weeks post the third immunization, mice ( $n=6$ ) were anaesthetized with ether and intranasally infected with 5 LD<sub>50</sub> of influenza A/Puerto Rico/8/1934 virus. All mice were monitored daily for morbidity and mortality for 14 days. Animals with 30% or greater body weight loss were euthanized immediately and considered as death.

## Quantification of Antibodies in Sera and BALF

The levels of antigen-specific antibodies in sera and bronchoalveolar lavage fluid (BALF) were quantified by enzyme-linked immunosorbent assay (ELISA). Blood samples ( $n=6$ ) were collected on days 0, 14, 28, and 35. BALF samples ( $n=5$ ) were collected 7 days after the third immunization. Briefly, the lungs from sacrificed mice were flushed three times with 1 ml PBS, which was then centrifuged at 3,500 g for 10 min. The supernatant was harvested for analysis of M2e-specific antibody titers. The ELISA plates were coated overnight at 4°C with 200 ng/well of M2e peptide pool consisting of equal amounts of peptides from human, swine, and avian influenza viruses or β-propiolactone-inactivated influenza A virus ( $1 \times 10^6$  PFU/well) or Hoc-Soc<sup>-</sup> T4 phages ( $1 \times 10^9$  PFU/well). The plates were blocked with 3% BSA in PBS-T (PBS containing 0.05% Tween-20) for 1 hour at 37°C. Serially diluted sera and BALF (1% BSA in PBS-T) were then added to each well of plates, which were incubated at 37°C for 1 hour. After washing 5 times with PBS-T, the plates were incubated with secondary antibodies (horseradish peroxidase-conjugated goat anti-mouse IgG, IgG1, IgG2a, and IgA) at 37°C for 1 hour. Following five washes, 100 µl of TMB (3,3',5,5'-tetramethylbenzidine) substrate was added to each well, and the reaction was stopped with 2 M H<sub>2</sub>SO<sub>4</sub>. The absorbance at OD<sub>450</sub> was determined by a microplate reader.

## Indirect Immunofluorescence Assay

About  $2 \times 10^5$  MDCK cells in 500 µl of growth medium (DMEM supplemented with 10% fetal bovine serum) were seeded into an each well of 24-well plate and allowed to adhere overnight. The growth medium was removed, and cells were washed twice with PBS and mock infected or infected with A/Puerto Rico/8/1934 virus in serum-free DMEM at a MOI of 1 for 1 h. The cells were then washed three times with PBS and cultured in serum-free DMEM containing 1 µg/ml TPCK-trypsin for 20h. After washing with PBS, cells were fixed with 10% formalin for 10 min, permeabilized with 0.1% Triton X-100 for 20 min, and blocked with 5% BSA in PBS-T (PBS containing 0.05% Tween-20) for 1 hour at 37 °C. The cells were then incubated with the sera from immunized mice at a dilution of 1:100 for 1h. After 5 times wash with PBS-T, Alexa Fluor 488 goat anti-mouse IgG (Thermo Fisher Scientific) were used as secondary antibodies at a dilution of 1:1000. Following five washes, nuclei were counterstained with 1 µg/ml DAPI (BD Biosciences) for 5 min in the dark. Photography was performed on an inverted fluorescence microscope (Thermo Fisher Scientific).

## Enzyme-Linked Immunosorbent Spot Assay

ELISPOT assay was performed to determine the number of M2e-specific IFN-γ and IL-4 secreting cells in spleen according to the manufacturer's protocol (DAKAWA, China). Briefly, 7 days post the last immunization, mice were sacrificed and the spleens were harvested to prepare single-cell suspensions. Around  $3 \times 10^5$  splenocytes were seeded to each well of plates and stimulated with M2e peptides (equal amounts of M2e peptide from human, swine, and avian influenza viruses) at a final concentration of 10 µg/ml. After 32-34 hours of culture at 37°C, 5% CO<sub>2</sub>, the splenocytes were removed by cell-cracking buffer of ice-cold deionized water. The plates were then incubated with biotinylated antibodies followed the addition of HRP-conjugated streptavidin. After washing 5 times, the reaction was developed with AEC (3-amino-9-ethylcarbazole) substrate and stopped with flowing water. Plates were dried at room temperature and spot-counted (DAKAWA, Wuhan, China).

## Histopathologic Analyses

Mice ( $n=3$ ) were immunized and challenged as described above. Five days after challenge with 5 LD<sub>50</sub> of influenza A/PR/8/1934 virus, mice were sacrificed, and lungs were isolated. Lung tissues were fixed in 10% formalin, dehydrated through a graded series of ethanol, embedded in paraffin wax, and cut into 4 µm-thick sections. After deparaffinization, sections were stained with hematoxylin-eosin and observed under an optical microscope (Nikon, Japan).

## Statistical Analysis

All the statistical analyses were performed using GraphPad Prism software. Comparisons among different groups were evaluated by one-way ANOVA. In all cases,  $p < 0.05$  was considered as statistically significant difference.

## DATA AVAILABILITY STATEMENT

The original contributions presented in the study are included in the article/**Supplementary Material**. Further inquiries can be directed to the corresponding authors.

## ETHICS STATEMENT

The animal study was reviewed and approved by The Research Ethics Committee (HZAUMO-2021-0023), Huazhong Agricultural University, Hubei, China.

## AUTHOR CONTRIBUTIONS

PT and ML designed the experiments. ML, PG, CC, and HF performed the experiments. ML, PG, WZ, and CG analyzed the data. ML, VR, and PT wrote the manuscript. PT directed

the project. All authors contributed to the article and approved the submitted version.

## FUNDING

This work was supported by grants from National Natural Science Foundation of China [Grant No. 31870915 to PT], Fundamental Research Funds for the Central Universities [Program No. 2662019

PY002 to PT], and in part by National Institute of Allergy and Infectious Diseases, National Institutes of Health [AI081726 to VR].

## SUPPLEMENTARY MATERIAL

The Supplementary Material for this article can be found online at: <https://www.frontiersin.org/articles/10.3389/fimmu.2021.745625/full#supplementary-material>

## REFERENCES

- Elbahesh H, Saletti G, Gerlach T, Rimmelzwaan GF. Broadly Protective Influenza Vaccines: Design and Production Platforms. *Curr Opin Virol* (2019) 34:1–9. doi: 10.1016/j.coviro.2018.11.005
- Monto AS, Fukuda K. Lessons From Influenza Pandemics of the Last 100 Years. *Clin Infect Dis* (2020) 70:951–7. doi: 10.1093/cid/ciz803
- Jang YH, Seong BL. The Quest for a Truly Universal Influenza Vaccine. *Front Cell Infect Microbiol* (2019) 9:344. doi: 10.3389/fcimb.2019.00344
- Sautto GA, Kirchenbaum GA, Ross TM. Towards a Universal Influenza Vaccine: Different Approaches for One Goal. *Virol J* (2018) 15:17. doi: 10.1186/s12985-017-0918-y
- Choi A, Bouzya B, Cortés Franco KD, Stadlbauer D, Rajabathor A, Rouxel RN, et al. Chimeric Hemagglutinin-Based Influenza Virus Vaccines Induce Protective Stalk-Specific Humoral Immunity and Cellular Responses in Mice. *ImmunoHorizons* (2019) 3:133–48. doi: 10.4049/immunohorizons.1900022
- Jang YH, Seong BL. Options and Obstacles for Designing a Universal Influenza Vaccine. *Viruses* (2014) 6:3159–80. doi: 10.3390/v6083159
- Nachbagauer R, Kinzler D, Choi A, Hirsh A, Beaulieu E, Lecrenier N, et al. A Chimeric Haemagglutinin-Based Influenza Split Virion Vaccine Adjuvanted With AS03 Induces Protective Stalk-Reactive Antibodies in Mice. *NPJ Vaccines* (2016) 1:16015–. doi: 10.1038/npjvaccines.2016.15
- Wong SS, Webby RJ. Traditional and New Influenza Vaccines. *Clin Microbiol Rev* (2013) 26:476–92. doi: 10.1128/CMR.00097-12
- Jazayeri SD, Poh CL. Development of Universal Influenza Vaccines Targeting Conserved Viral Proteins. *Vaccines* (2019) 7:169. doi: 10.3390/vaccines7040169
- Sah P, Alfaro-Murillo JA, Fitzpatrick MC, Neuzil KM, Meyers LA, Singer BH, et al. Future Epidemiological and Economic Impacts of Universal Influenza Vaccines. *Proc Natl Acad Sci USA* (2019) 116:20786–92. doi: 10.1073/pnas.1909613116
- Webster RG, Govorkova EA. Continuing Challenges in Influenza. *Ann New Y Acad Sci* (2014) 1323:115–39. doi: 10.1111/nyas.12462
- Wei CJ, Crank MC, Shiver J, Graham BS, Mascola JR, Nabel GJ. Next-Generation Influenza Vaccines: Opportunities and Challenges. *Nat Rev Drug Discov* (2020) 19:239–52. doi: 10.1038/s41573-019-0056-x
- Pica N, Palese P. Toward a Universal Influenza Virus Vaccine: Prospects and Challenges. *Annu Rev Med* (2013) 64:189–202. doi: 10.1146/annurev-med-120611-145115
- Nachbagauer R, Palese P. Is a Universal Influenza Virus Vaccine Possible? *Annu Rev Med* (2020) 71:315–27. doi: 10.1146/annurev-med-120617-041310
- Herrera-Rodriguez J, Meijerhof T, Niesters HG, Stjernholm G, Hovden AO, Sorensen B, et al. A Novel Peptide-Based Vaccine Candidate With Protective Efficacy Against Influenza A in a Mouse Model. *Virology* (2018) 515:21–8. doi: 10.1016/j.virol.2017.11.018
- Li ZT, Zarnitsyna VI, Lowen AC, Weissman D, Koelle K, Kohlmeier JE, et al. Why Are CD8 T Cell Epitopes of Human Influenza A Virus Conserved? *J Virol* (2019) 93:e01534-18. doi: 10.1128/JVI.01534-18
- Pleguezuelos O, James E, Fernandez A, Lopes V, Rosas LA, Cervantes-Medina A, et al. Efficacy of FLU-V, a Broad-Spectrum Influenza Vaccine, in a Randomized Phase IIb Human Influenza Challenge Study. *NPJ Vaccines* (2020) 5:22. doi: 10.1038/s41541-020-0174-9
- Krammer F. The Quest for a Universal Flu Vaccine: Headless HA 2.0. *Cell Host Microbe* (2015) 18:395–7. doi: 10.1016/j.chom.2015.10.003
- Li CK, Rappuoli R, Xu XN. Correlates of Protection Against Influenza Infection in Humans—on the Path to a Universal Vaccine? *Curr Opin Immunol* (2013) 25:470–6. doi: 10.1016/j.coi.2013.07.005
- Sei CJ, Rao M, Schuman RF, Daum LT, Matyas GR, Rikhi N, et al. Conserved Influenza Hemagglutinin, Neuraminidase and Matrix Peptides Adjuvanted With ALFQ Induce Broadly Neutralizing Antibodies. *Vaccines* (2021) 9:698. doi: 10.3390/vaccines9070698
- Zharikova D, Mozdzanowska K, Feng J, Zhang M, Gerhard W. Influenza Type A Virus Escape Mutants Emerge *In Vivo* in the Presence of Antibodies to the Ectodomain of Matrix Protein 2. *J Virol* (2005) 79:6644–54. doi: 10.1128/JVI.79.11.6644-6654.2005
- Deng L, Mohan T, Chang TZ, Gonzalez GX, Wang Y, Kwon YM, et al. Double-Layered Protein Nanoparticles Induce Broad Protection Against Divergent Influenza A Viruses. *Nat Commun* (2018) 9:359. doi: 10.1038/s41467-017-02725-4
- Fiers W, De Filette M, El Bakkouri K, Schepens B, Roose K, Schotsaert M, et al. M2e-Based Universal Influenza A Vaccine. *Vaccine* (2009) 27:6280–3. doi: 10.1016/j.vaccine.2009.07.007
- He F, Leyrer S, Kwang J. Strategies Towards Universal Pandemic Influenza Vaccines. *Expert Rev Vaccines* (2016) 15:215–25. doi: 10.1586/14760584.2016.1115352
- Ibañez LI, Roose K, De Filette M, Schotsaert M, De Sloovere J, Roels S, et al. M2e-Displaying Virus-Like Particles With Associated RNA Promote T Helper 1 Type Adaptive Immunity Against Influenza A. *PLoS One* (2013) 8:e59081. doi: 10.1371/journal.pone.0059081
- Tao P, Mahalingam M, Kirtley ML, van Lier CJ, Sha J, Yeager LA, et al. Mutated and Bacteriophage T4 Nanoparticle Arrayed F1-V Immunogens From *Yersinia Pestis* as Next Generation Plague Vaccines. *PLoS Pathog* (2013) 9:e1003495. doi: 10.1371/journal.ppat.1003495
- Tao P, Mahalingam M, Zhu J, Moayeri M, Sha J, Lawrence WS, et al. A Bacteriophage T4 Nanoparticle-Based Dual Vaccine Against Anthrax and Plague. *mBio* (2018) 9:e01926-18. doi: 10.1128/mBio.01926-18
- Schepens B, De Vlieger D, Saelens X. Vaccine Options for Influenza: Thinking Small. *Curr Opin Immunol* (2018) 53:22–9. doi: 10.1016/j.coi.2018.03.024
- Kim KH, Kwon YM, Lee YT, Kim MC, Hwang HS, Ko EJ, et al. Virus-Like Particles Are a Superior Platform for Presenting M2e Epitopes to Prime Humoral and Cellular Immunity Against Influenza Virus. *Vaccines* (2018) 6:66. doi: 10.3390/vaccines6040066
- Tao W, Hurst BL, Shakyia AK, Uddin MJ, Ingrole RS, Hernandez-Sanabria M, et al. Consensus M2e Peptide Conjugated to Gold Nanoparticles Confers Protection Against H1N1, H3N2 and H5N1 Influenza A Viruses. *Antiviral Res* (2017) 141:62–72. doi: 10.1016/j.antiviral.2017.01.021
- Neiryck S, Deroo T, Saelens X, Vanlandschoot P, Jou WM, Fiers W. A Universal Influenza A Vaccine Based on the Extracellular Domain of the M2 Protein. *Nat Med* (1999) 5:1157–63. doi: 10.1038/13484
- Matić S, Rinaldi R, Masenga V, Noris E. Efficient Production of Chimeric Human Papillomavirus 16 L1 Protein Bearing the M2e Influenza Epitope in *Nicotiana Benthamiana* Plants. *BMC Biotechnol* (2011) 11:106. doi: 10.1186/1472-6750-11-106
- Petukhova NV, Gasanova TV, Stepanova LA, Rusova OA, Potapchuk MV, Korotkov AV, et al. Immunogenicity and Protective Efficacy of Candidate Universal Influenza A Nanovaccines Produced in Plants by Tobacco Mosaic Virus-Based Vectors. *Curr Pharm Des* (2013) 19:5587–600. doi: 10.2174/13816128113199990337



34. Hashemi H, Pouyanfar S, Bandehpour M, Noroozbabaei Z, Kazemi B, Saelens X, et al. Immunization With M2e-Displaying T7 Bacteriophage Nanoparticles Protects Against Influenza A Virus Challenge. *PLoS One* (2012) 7:e45765. doi: 10.1371/journal.pone.0045765
35. Kim MC, Lee JS, Kwon YM, O E, Lee YJ, Choi JG, et al. Multiple Heterologous M2 Extracellular Domains Presented on Virus-Like Particles Confer Broader and Stronger M2 Immunity Than Live Influenza A Virus Infection. *Antiviral Res* (2013) 99:328–35. doi: 10.1016/j.antiviral.2013.06.010
36. Liu W, Peng Z, Liu Z, Lu Y, Ding J, Chen YH. High Epitope Density in a Single Recombinant Protein Molecule of the Extracellular Domain of Influenza A Virus M2 Protein Significantly Enhances Protective Immunity. *Vaccine* (2004) 23:366–71. doi: 10.1016/j.vaccine.2004.05.028
37. Cheng W. The Density Code for the Development of a Vaccine? *J Pharm Sci* (2016) 105:3223–32. doi: 10.1016/j.xphs.2016.07.020
38. Tao P, Zhu J, Mahalingam M, Batra H, Rao VB. Bacteriophage T4 Nanoparticles for Vaccine Delivery Against Infectious Diseases. *Adv Drug Deliv Rev* (2019) 145:57–72. doi: 10.1016/j.addr.2018.06.025
39. Deng L, Ibañez LI, Van den Bossche V, Roose K, Youssef SA, de Bruin A, et al. Protection Against Influenza A Virus Challenge With M2e-Displaying Filamentous Escherichia Coli Phages. *PLoS One* (2015) 10:e0126650. doi: 10.1371/journal.pone.0126650
40. Tao P, Mahalingam M, Marasa BS, Zhang Z, Chopra AK, Rao VB. *In Vitro* and *In Vivo* Delivery of Genes and Proteins Using the Bacteriophage T4 DNA Packaging Machine. *Proc Natl Acad Sci USA* (2013) 110:5846–51. doi: 10.1073/pnas.1300867110
41. Tao P, Wu X, Tang WC, Zhu J, Rao V. Engineering of Bacteriophage T4 Genome Using CRISPR-Cas9. *ACS Synth Biol* (2017) 6:1952–61. doi: 10.1021/acssynbio.7b00179
42. Sathaliyawala T, Rao M, Maclean DM, Birx DL, Alving CR, Rao VB. Assembly of Human Immunodeficiency Virus (HIV) Antigens on Bacteriophage T4: A Novel *in vitro* Approach to Construct Multicomponent HIV Vaccines. *J Virol* (2006) 80:7688–98. doi: 10.1128/JVI.00235-06
43. Shivachandra SB, Li Q, Peachman KK, Matyas GR, Leppla SH, Alving CR, et al. Multicomponent Anthrax Toxin Display and Delivery Using Bacteriophage T4. *Vaccine* (2007) 25:1225–35. doi: 10.1016/j.vaccine.2006.10.010
44. Tao P, Li Q, Shivachandra SB, Rao VB. Bacteriophage T4 as a Nanoparticle Platform to Display and Deliver Pathogen Antigens: Construction of an Effective Anthrax Vaccine. *Methods Mol Biol (Clifton NJ)* (2017) 1581:255–67. doi: 10.1007/978-1-4939-6869-5\_15
45. Boudreau CM, Alter G. Extra-Neutralizing FcR-Mediated Antibody Functions for a Universal Influenza Vaccine. *Front Immunol* (2019) 10:440. doi: 10.3389/fimmu.2019.00440
46. Deloizy C, Fossum E, Barnier-Quer C, Urien C, Chrun T, Duval A, et al. The Anti-Influenza M2e Antibody Response Is Promoted by XCR1 Targeting in Pig Skin. *Sci Rep* (2017) 7:7639. doi: 10.1038/s41598-017-07372-9
47. Sedova ES, Scherbinin DN, Lysenko AA, Alekseeva SV, Artemova EA, Shmarov MM. Non-Neutralizing Antibodies Directed at Conservative Influenza Antigens. *Acta Naturae* (2019) 11:22–32. doi: 10.32607/20758251-2019-11-4-22-32
48. Qi M, Zhang XE, Sun X, Zhang X, Yao Y, Liu S, et al. Intranasal Nanovaccine Confers Homo- and Hetero-Subtypic Influenza Protection. *Small (Weinheim an der Bergstrasse Germany)* (2018) 14:e1703207. doi: 10.1002/smll.201703207
49. Eliasson DG, Omokanye A, Schön K, Wenzel UA, Bernasconi V, Bemark M, et al. M2e-Tetramer-Specific Memory CD4 T Cells Are Broadly Protective Against Influenza Infection. *Mucosal Immunol* (2018) 11:273–89. doi: 10.1038/mi.2017.14
50. Mezhsenskaya D, Isakova-Sivak I, Rudenko L. M2e-Based Universal Influenza Vaccines: A Historical Overview and New Approaches to Development. *J BioMed Sci* (2019) 26:76. doi: 10.1186/s12929-019-0572-3
51. Saelens X. The Role of Matrix Protein 2 Ectodomain in the Development of Universal Influenza Vaccines. *J Infect Dis* (2019) 219:S68–s74. doi: 10.1093/infdis/jiz003
52. Sun X, Wang Y, Dong C, Hu J, Yang L. High Copy Numbers and N Terminal Insertion Position of Influenza A M2E Fused With Hepatitis B Core Antigen Enhanced Immunogenicity. *Biosci Trends* (2015) 9:221–7. doi: 10.5582/bst.2015.01060
53. Gomes AC, Flace A, Saudan P, Zabel F, Cabral-Miranda G, Turabi AE, et al. Adjusted Particle Size Eliminates the Need of Linkage of Antigen and Adjuvants for Appropriated T Cell Responses in Virus-Like Particle-Based Vaccines. *Front Immunol* (2017) 8:226. doi: 10.3389/fimmu.2017.00226
54. Azouz A, Razzaque MS, El-Hallak M, Taguchi T. Immunoinflammatory Responses and Fibrogenesis. *Med Electron Microsc* (2004) 37:141–8. doi: 10.1007/s00795-004-0255-2
55. Berger A. Th1 and Th2 Responses: What are They? *BMJ (Clin Res ed)* (2000) 321:424. doi: 10.1136/bmj.321.7258.424
56. Li X, Xing R, Xu C, Liu S, Qin Y, Li K, et al. Immunostimulatory Effect of Chitosan and Quaternary Chitosan: A Review of Potential Vaccine Adjuvants. *Carbohydr Polymers* (2021) 264:118050. doi: 10.1016/j.carbpol.2021.118050
57. Von Holle TA, Moody MA. Influenza and Antibody-Dependent Cellular Cytotoxicity. *Front Immunol* (2019) 10:1457. doi: 10.3389/fimmu.2019.01457
58. Kim MC, Lee YN, Ko EJ, Lee JS, Kwon YM, Hwang HS, et al. Supplementation of Influenza Split Vaccines With Conserved M2 Ectodomains Overcomes Strain Specificity and Provides Long-Term Cross Protection. *Mol Ther* (2014) 22:1364–74. doi: 10.1038/mt.2014.33
59. Tao P, Mahalingam M, Rao VB. Highly Effective Soluble and Bacteriophage T4 Nanoparticle Plague Vaccines Against Yersinia Pestis. *Methods Mol Biol (Clifton NJ)* (2016) 1403:499–518. doi: 10.1007/978-1-4939-3387-7\_28
60. Zhu J, Ananthaswamy N, Jain S, Batra H, Tang WC, Lewry DA, et al. A Universal Bacteriophage T4 Nanoparticle Platform to Design Multiplex SARS-CoV-2 Vaccine Candidates by CRISPR Engineering. *Sci Adv* (2021) 7:eabh1547. doi: 10.1126/sciadv.abh1547
61. Brito LA, Singh M. Acceptable Levels of Endotoxin in Vaccine Formulations During Preclinical Research. *J Pharm Sci* (2011) 100:34–7. doi: 10.1002/jps.22267

**Conflict of Interest:** The authors declare that the research was conducted in the absence of any commercial or financial relationships that could be construed as a potential conflict of interest.

**Publisher's Note:** All claims expressed in this article are solely those of the authors and do not necessarily represent those of their affiliated organizations, or those of the publisher, the editors and the reviewers. Any product that may be evaluated in this article, or claim that may be made by its manufacturer, is not guaranteed or endorsed by the publisher.

Copyright © 2021 Li, Guo, Chen, Feng, Zhang, Gu, Wen, Rao and Tao. This is an open-access article distributed under the terms of the Creative Commons Attribution License (CC BY). The use, distribution or reproduction in other forums is permitted, provided the original author(s) and the copyright owner(s) are credited and that the original publication in this journal is cited, in accordance with accepted academic practice. No use, distribution or reproduction is permitted which does not comply with these terms.